POAC'15
Trondheim, Norway
Port and Ocean Engineering under Arctic Conditions
June 14-18, 2015
Trondheim, Norway

2D DEM OF ICE RUBBLE: THE EFFECT OF RATE-DEPENDENT FRICTION

Ben Lishman [1] and Arttu Polojärvi [2,3]
[1] University College London, WC1E6BT, London, UK
[2] Aalto University, School of Engineering, Department of Applied Mechanics
P.O. Box 14300, FI-00076 Aalto, Finland
[3] Sustainable Arctic Marine and Coastal Technology (SAMCoT), Centre for Research-based Innovation (CRI), Norwegian University of Science and Technology, Trondheim, Norway
email: b.lishman@ucl.ac.uk

ABSTRACT
The friction coefficient of ice on ice is usually modeled as a constant. However, theory and experimental data show that ice-ice friction depends on the speed of sliding. In this paper we incorporate a rate-dependent friction coefficient into 2D discrete element method simulations of ice ensemble behaviour. Friction is high (0.7) at low sliding speeds ($<10^{-6}$ ms^{-1}), low (0.1) at high sliding speeds ($>10^{-2}$ ms^{-1}) and decreases log-linearly between these values. We show qualitatively and quantitatively how this affects the overall dynamics of a shear box experiment.

INTRODUCTION
To understand and predict the behaviour of large ensembles of ice, it is useful to be able to model the interactions between ice blocks. Comprehensive modeling of ice mass (either rubble or ice pack consisting of numerous ice floes) is achieved using the discontinuous approach. In this type of modeling each individual ice block or floe in the ice mass is modeled, and it is the motion and the interaction of them that causes the deformation of the ice mass under loading. In this paper we will do this type of modeling using the discrete element method (DEM). A similar type of approach was used by Hopkins (1996, 2004) and Hopkins and Thorndike (2006), who derived sea ice ridging resistance from a small-scale DEM model, and used this resistance as a parameter for a large-scale DEM model of full Arctic ice pack.

If we want to know the forces between ice blocks, we must know, amongst other things, the *friction* between the blocks – the ratio of tangential force to normal force at contacts between blocks. Typically this ratio, μ, is modeled as a constant in DEM: Hopkins (1996) investigates a range from 0.1 to 0.8 for the coefficient of friction, but uses a single value within any individual experiment.

Experimental evidence suggests that the friction of ice on ice is not constant. In this paper we are particularly interested in the *rate-dependence* of friction: put simply, that the ice-ice friction coefficient depends on the sliding speed. This rate dependence is one source of the variability of friction coefficient: μ appears to have a peak of around 0.7 at low sliding speeds, dropping to 0.1 at high sliding speeds. Figure 1, based on Maeno et al (2003) shows a range of experimentally determined values.

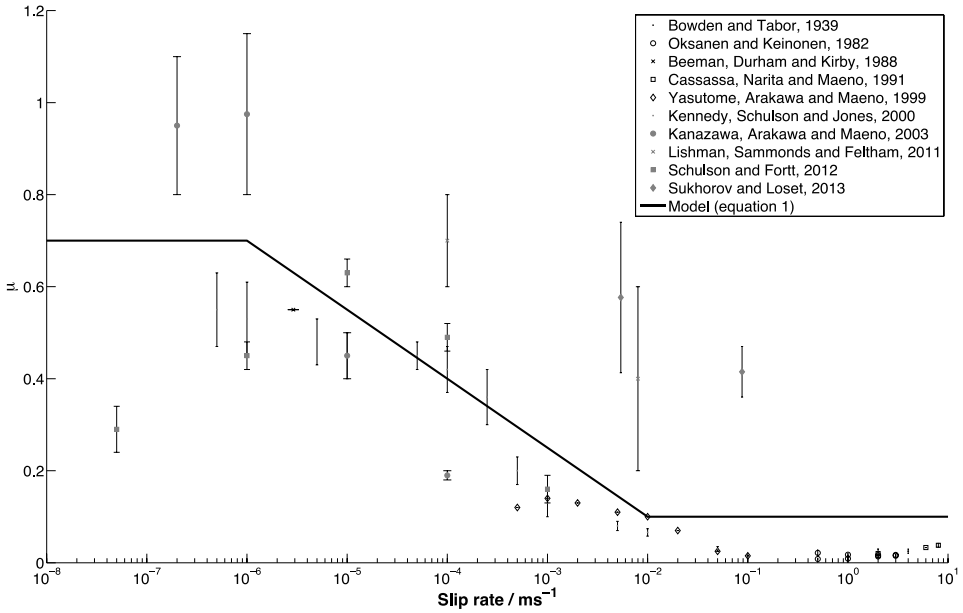

Figure 1. Experimentally determined values for ice-ice friction (after Maeno et al., 2003), with a simple rate-dependent friction model (described in the text by equation 1) overlaid.

Our proposed friction model is overlaid on figure 1. The model has three regimes:

$$v_s <= 10^{-6}\,ms^{-1} \qquad \mu = 0.7 \qquad (1a)$$

$$10^{-6}\,ms^{-1} < v_s < 10^{-2}\,ms^{-1} \qquad \mu = 0.1 - 0.15\,log_{10}(100v_s) \qquad (1b)$$

$$v_s >= 10^{-2}\,ms^{-1} \qquad \mu = 0.1 \qquad (1c)$$

This friction model is easy to understand and introduces only minor additional computational complexity, whilst providing a reasonable match to available experimental data. We note here that experimental data measured in the laboratory may not fully reflect processes which affect sea ice friction in the field (Hopkins 1996), but we also note that the results shown in figure 1 include field measurements and ice tank measurements, which follow the general trends of the small-scale experiments.

Previous DEM work has assumed a constant friction coefficient, which would be represented by a horizontal line on figure 1. In this preliminary modelling work on this topic, we investigate how a simple discrete element model responds to the rate-dependent friction model of equation 1. In general we compare this model to three other constant-friction cases - $\mu = 0.1$, $\mu = 0.4$, and $\mu = 0.7$ – which represent the minimum, midpoint and maximum of the bold line overlaid on figure 1.

METHOD: SIMULATIONS

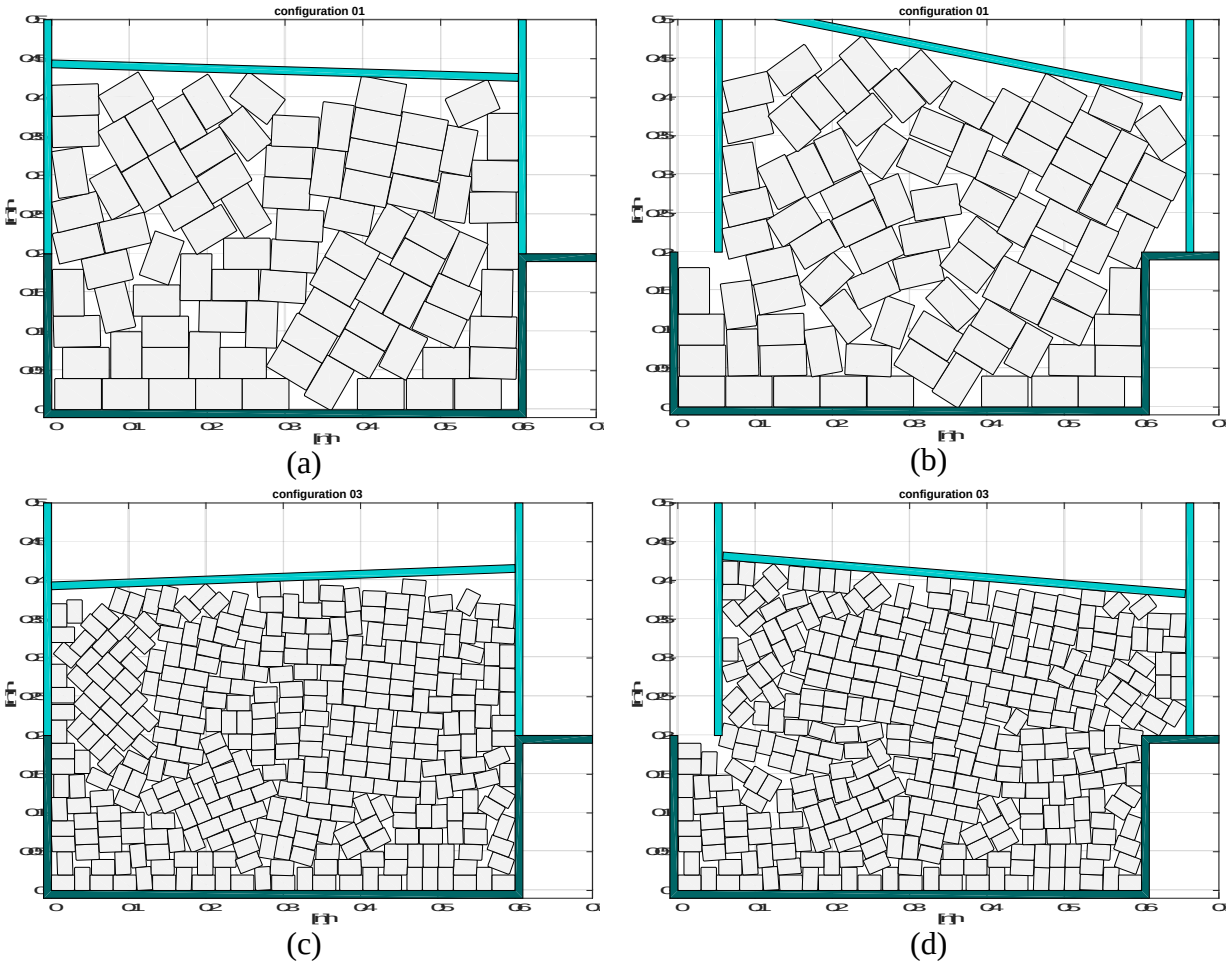

(a) (b) (c) (d)

Figure 2**.** Direct shear box simulation: the top half of the shear box is moved 6cm from left to right. Images (a) and (b) show the simulation with larger (6x4cm) blocks in its initial and final states. Similarly, (c) and (d) show the simulation with smaller blocks (2x3cm) in its initial and final states.

Our two dimensional discrete element method (DEM) simulations are largely based on the models described in detail in Hopkins (1992) and Paavilainen et al. (2009). The normal forces in contact are always compressive: in other words, there are no freeze bonds between the blocks. The block fracture is not modelled. The contact forces between the blocks are calculated using an elastic-viscous-plastic normal force model and an incremental rate-dependent Mohr–Coulomb tangential force model. The rate-dependency is modeled by changing the friction coefficient value according to equation 1, with the relative tangential speed of the blocks at the point of contact used as sliding velocity v_s. The main parameters used in the simulations are given in Table 1.

Figure 2 and 3 illustrate the simulation set-up. The set-up was based on pseudo 2D shear box experiments described in detail in Pustogvar et al. (2014). The rubble specimen inside the box had a length L=0.6 m and the height H=0.4 m. A solid cover applied confining pressure σ_n onto the rubble. The cover was free to rotate and move in the vertical direction, leading to

constant σ_n during an experiment. The σ_n value used in the simulations was 5.76 kPa. The velocity of the box motion was set up to 20 mms^{-1}. The upper half of the boxed moved through the displacement interval 0…0.06m, over a period of 3s in the simulations. Simulations with two different sizes of rubble blocks were performed: small 2x3cm blocks and large 4x6cm blocks.

Table 1. Main parameters used in the simulations.

Parameter		*Unit*	*Value*	*Parameter*		*Unit*	*Value*
Ice-ice friction coefficient	μ_{ii}		variable	Rubble length	L	m	0.6
Ice-wall friction coefficient	μ_{iw}		equal to μ_{ii}	Rubble height	H	m	0.4
Normal contact stiffness	-	Pa	$4.0 \bullet 10^8$	Shearing velocity	$\dot{\delta}$	ms^{-1}	0.02
Tangential contact stiffness	-	Pa	$1.5 \bullet 10^8$	Confining pressure	σ_n	kPa	5.76
Plastic limit	-	Pa	$2.0 \bullet 10^8$	Small block size	-	m × m	0.02×0.03
				Large block size	-	m × m	0.04×0.06

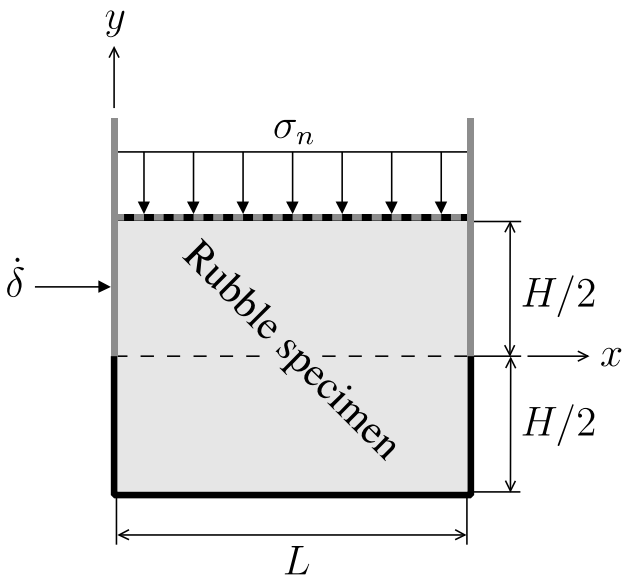

Figure 3. A sketch of the shear box simulation showing symbols used in the text.

RESULTS

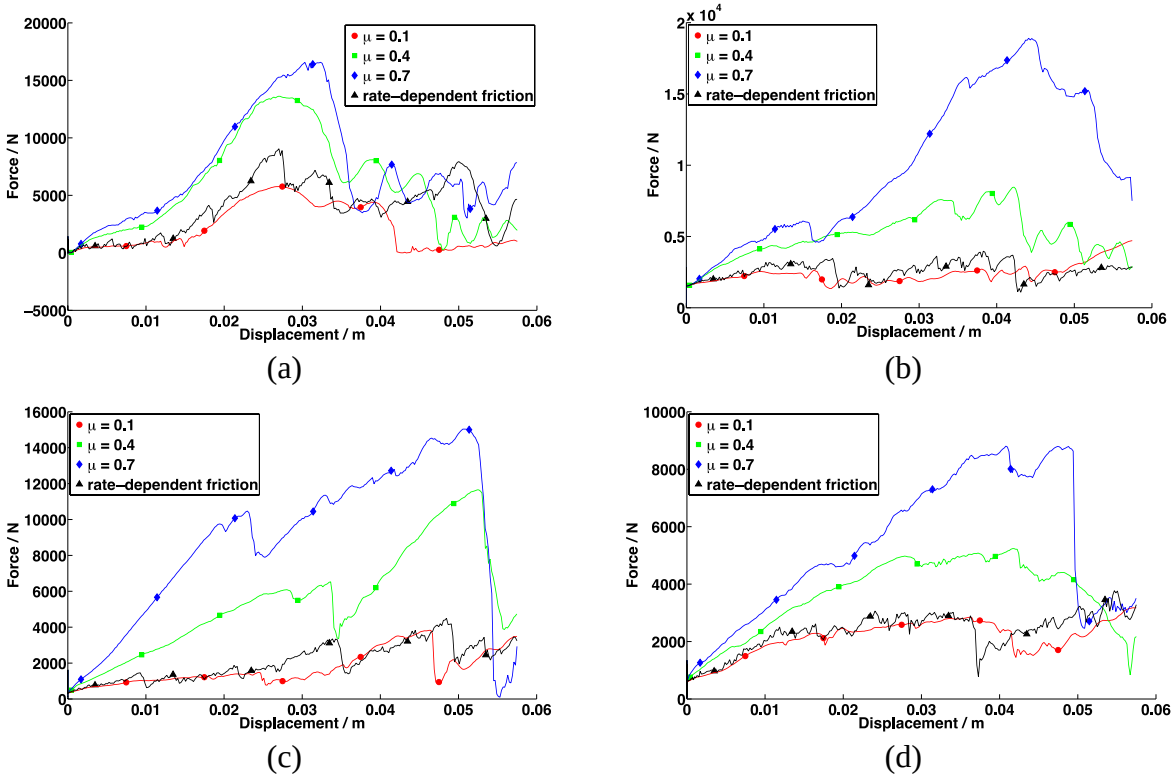

Figure 4. Plots of force against displacement for four shear box simulations with various friction models. Plots (a) and (b) show results for simulations with large blocks, differing only in their initial configuration. Plots (c) and (d) show results for simulations with small blocks, and again differ only in their initial block arrangement. In each plot, the red line marked with circles shows the forces with $\mu = 0.1$, the green line marked with squares shows the forces with $\mu = 0.4$, the blue line marked with diamonds shows the forces with $\mu = 0.7$, and the black line marked with triangles shows the forces with rate-dependent friction (see equation 1).

Figure 4 shows the simulated force required to move the top half of the shear box, as a function of displacement. The three constant friction models (red, green and blue lines) show increased shear force with increased ice-ice friction, as might be expected. The rate-dependent friction model shows low forces, comparable to those with $\mu = 0.1$. Also, notably, in each case the loads with rate-dependent friction show more saw-tooth behaviour, whereas the constant friction results (particularly with low friction) show smoother results.

It is potentially interesting to understand how these forces are supported by individual block-block interactions. One attempt to visualize this is shown in figure 5. Figure 5 shows results for configuration 1, with large blocks, only, but similar results hold for the other configurations tested. To create figure 5, we take each interaction in each timestep, and find the energy dissipated in that interaction (tangential force x tangential speed x Δt). We then plot this energy, summed over all timesteps and all interactions, as a function of tangential force and tangential speed. This allows us to see what kinds of interactions are dissipating the most energy. For $\mu = 0.1$, at the top right of figure 5, energy is dissipated mostly in fast sliding ($v>10^{-3}$): the darkest region is towards the right of the graph. For $\mu = 0.7$, energy is

also dissipated at lower speeds (down to $v=10^{-5}$) but higher loads. It seems noteworthy that the plot for rate-dependent friction is most similar to that for $\mu = 0.7$; i.e. the dark, high-energy section of the graph extents to lower speeds than that for $\mu = 0.1$. We also note that the model with rate-dependent friction tends to devolve into two separate regions of high energy interactions - a low-speed cloud around $\{v = 10^{-4}, F = 10^{2}\}$ and a high-speed cloud around $\{v = 10^{-2}, F=10^{1}\}$. These high-energy zones don't meet on the plot; they are separated by a lower-energy zone. Perhaps the sliding states of some interactions are at high speed and low force, and other interactions at low speed and high force. An alternative hypothesis is that block-block interactions oscillate between the two states. Understanding how the two states arise might allow us to understand the sawtooth behaviour seen on the rate-dependent friction force plot (black lines) in figure 4.

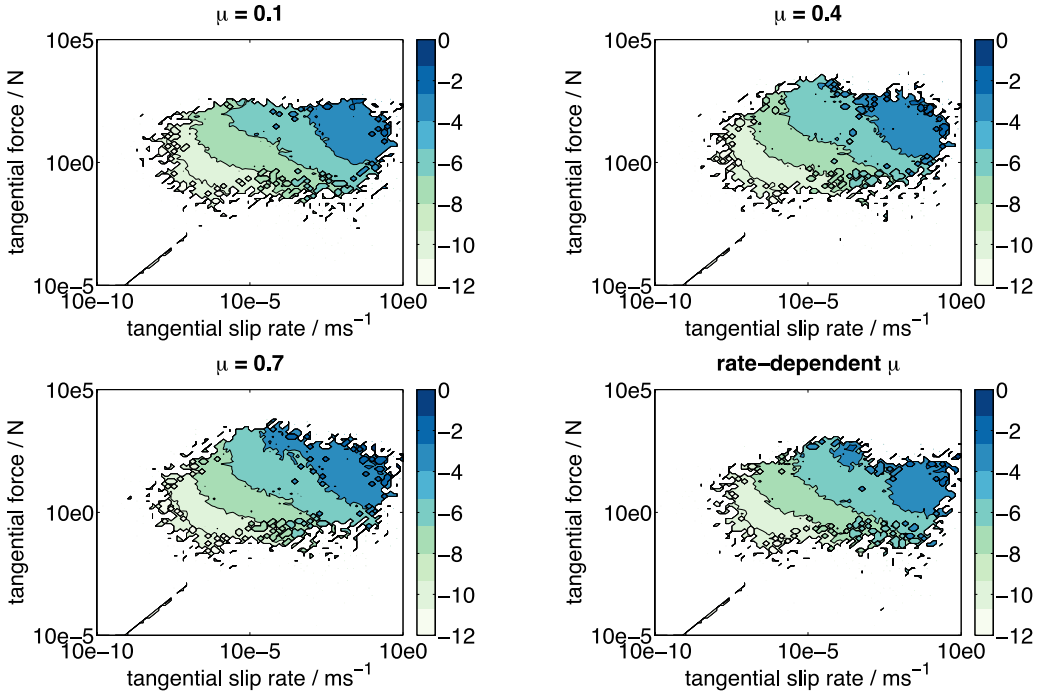

Figure 5. Plots of energy distribution as a function of block-block slip rate and tangential force. In each case, the energy generated at each interaction and each timestep is calculated, and summed over the whole simulation. Darker areas represent more energy dissipation, while white areas represent regions in which no events occur. The upper left plot shows results for $\mu = 0.1$, the upper right for $\mu = 0.4$, the lower left for $\mu = 0.7$, and the lower right for rate-dependent friction.

DISCUSSION AND CONCLUSIONS

We have attempted to make a preliminary systematic analysis of how choice of friction model affects the results of a DEM model of a shear box full of ice rubble. We hope that in the future this analysis will also help us understand how choice of friction model affects DEMs more broadly. Within our shear box experiments, we find three results which were not necessarily expected:

1) *From figure 4.* Forces required to move the shear box, or to deform the ice ensemble, are comparable between the rate-dependent model and the lowest value ($\mu = 0.1$) of constant friction. This might suggest that the overall forces are controlled by the high speed interactions ($v>10^{-2}$), since for these interactions $\mu = 0.1$ in the rate-dependent case. Overall forces with $\mu = 0.4$ and $\mu = 0.7$ are considerably higher.
2) *From figure 4.* These forces show a noticeable sawtooth behaviour in the rate-dependent case which is not present with $\mu = 0.1$. In fact, this sawtooth behaviour seems clearer in the rate-dependent case than in any other.
3) *From figure 5.* The energy dissipation in the rate-dependent case appears to be divided between two separate regimes: one at low speed/high load and one at high speed/low load. Somewhat similar behaviour is seen with high constant friction, but not with the low friction case.

To sum this up in one sentence: for the experiment outlined above, rate-dependent friction is like $\mu = 0.1$ in its effect on the *magnitude* of the forces, but like $\mu = 0.7$ in its effect on the *nature* of the forces. If this result were true of ice interactions in general, then it would lead to the conclusion that the rate-dependent effects of ice friction cannot be successfully modelled by any single value of μ.

Two important limits apply to this study.

1) Our field of investigation so far includes one shear box experiment. It seems important to see how these results scale to different numbers of interactions (e.g. large rubble piles), and across different block sizes (e.g. metre-scale). This is our next focus.
2) These results are only useful insofar as they represent some physical reality. Ideally they would be validated against experiments on ice.

In conclusion, we have conducted a preliminary series of DEM shear box simulations to model the effects of allowing block-block friction to vary with block-block sliding speed. This rate-dependent variability of friction seems to be supported by a range of experimental and theoretical data. The overall effect on our shear box experiment is that the new friction model causes similar force magnitudes to those with low ice-ice friction, but this force is less smooth. Early evidence suggests that two separate sliding states dominate the energy dissipation.

ACKNOWLEDGMENTS

Both authors would like to thank the European Science Foundation for funding travel for this collaboration under their programme "Micro-dynamics of ice." AP wishes to acknowledge the support from the Research Council of Norway through the Centre for Research-based Innovation SAMCoT and the support from all SAMCoT partners.

REFERENCES

Beeman, M., Durham, W. B., & Kirby, S. H., 1988. Friction of ice. *Journal of Geophysical Research: Solid Earth (1978–2012)*, *93*(B7), 7625-7633.

Bowden, F. P., & Tabor, D., 1939. The area of contact between stationary and between moving surfaces. *Proceedings of the Royal Society of London. Series A, Mathematical and Physical Sciences*, 391-413.

Casassa, G., Narita, H., & Maeno, N., 1991. Shear cell experiments of snow and ice friction. *Journal of applied physics*, *69*(6), 3745-3756.

Hopkins, M., 1992. Numerical simulation of systems of multitudinous polygonal blocks. Tech- nical Report 92-22, Cold Regions Research and Engineering Laboratory, CRREL. 69 p.

Kanazawa, S., Arakawa, M., & Maeno, N., 2003. Measurements of ice-ice friction coefficients at low sliding velocities. *Seppyo*, *65*(4), 389-397.

Kennedy, F. E., Schulson, E. M., & Jones, D. E., 2000. The friction of ice on ice at low sliding velocities. *Philosophical Magazine A*, *80*(5), 1093-1110.

Lishman, B., Sammonds, P., & Feltham, D., 2011. A rate and state friction law for saline ice. *Journal of Geophysical Research: Oceans (1978–2012)*, *116*(C5).

Maeno, N., Arakawa, M., Yasutome, A., Mizukami, N., & Kanazawa, S., 2003. Ice ice friction measurements, and water lubrication and adhesion-shear mechanisms. *Canadian journal of physics*, *81*(1-2), 241-249.

Oksanen, P., & Keinonen, J., 1982. The mechanism of friction of ice. *Wear*,*78*(3), 315-324.

Paavilainen, J., Tuhkuri, J., and Polojärvi, A., 2009. 2D combined finite–discrete element method to model multi-fracture of beam structures. *Engineering Computations*, 26(6):578–598.

Pustogvar, A., Høyland, K. V., Polojärvi, A., and Bueide, I. M., 2014. Laboratory scale direct shear box experiments on ice rubble: the effect of block to box size ratio. In *Proceedings of OMAE14, 33th International Conference On Offshore Mechanics and Artcic Engineering*.

Schulson, E. M., & Fortt, A. L., 2012. Friction of ice on ice. *Journal of Geophysical Research: Solid Earth (1978–2012)*, *117*(B12).

Sukhorukov, S., & Løset, S., 2013. Friction of sea ice on sea ice. *Cold Regions Science and Technology*, *94*, 1-12.

Yasutome, A., Arakawa, M., & Maeno, N., 1999. Measurements of ice-ice friction coefficients. *Seppyo*, *61*(6), 437-443.